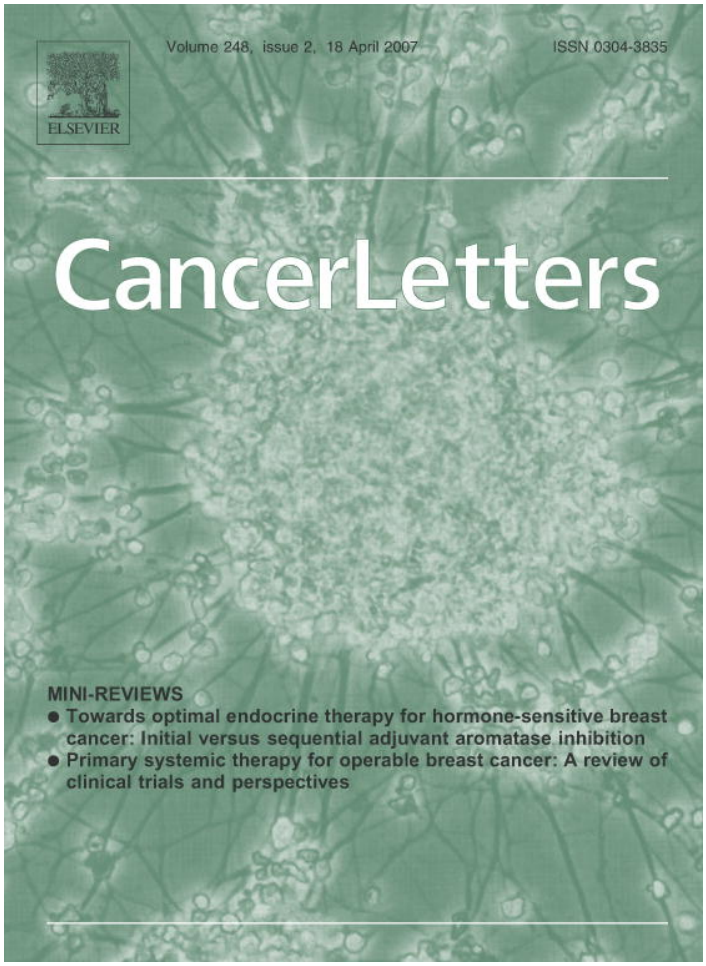

Available online at www.sciencedirect.com
ScienceDirect
Cancer Letters 248 (2007) 198–210
CANCER Letters
www.elsevier.com/locate/canlet

The TCL1 oncoprotein binds the RNase PH domains of the PNPase exoribonuclease without affecting its RNA degrading activity

Samuel W. French [a], David W. Dawson [a], Hsiao-Wen Chen [a], Robert N. Rainey [b], Stuart A. Sievers [b], Cynthia E. Balatoni [a], Larry Wong [a], Joshua J. Troke [a], Mai T.N. Nguyen [a], Carla M. Koehler [b,c], Michael A. Teitell [a,c,*]

[a] *Department of Pathology and Laboratory Medicine, David Geffen School of Medicine at UCLA, Los Angeles, CA 90095-1732, USA*
[b] *Department of Chemistry and Biochemistry, UCLA, Los Angeles, CA 90095-1569, USA*
[c] *Molecular Biology Institute and Jonsson Comprehensive Cancer Center, UCLA, Los Angeles, CA 90095, USA*

Received 12 April 2006; accepted 13 July 2006

Abstract

TCL1 is an AKT kinase coactivator that, when dysregulated, initiates mature lymphocyte malignancies in humans and transgenic mice. While TCL1 augments AKT pathway signaling, additional TCL1 interacting proteins that may contribute to cellular homeostasis or transformation are lacking. Here, an exoribonuclease, PNPase, was identified in a complex with TCL1. The AKT interaction domain on TCL1 bound either RNase PH repeat domain of PNPase without influencing its RNA degrading activity, which was compatible with predicted docking models for a TCL1–PNPase complex. Our data provide a novel protein interaction for mammalian PNPase that may impact TCL1 mediated transformation.

Keywords: TCL1; PNPase; Exoribonuclease; Mass spectrometry; Leukemia; Lymphoma

1. Introduction

T cell leukemia-1 (TCL1) is a 14-kDa intracellular oncoprotein that when dysregulated by heightened or continuous expression is implicated in the development of mature B and T cell leukemias and lymphomas in humans and transgenic mice (reviewed in [1]). TCL1 is non-enzymatic and its only known binding partner is the AKT (protein kinase B) serine/threonine kinase [2]. The interaction of TCL1 with AKT causes a modest increase in pre-activated AKT phosphorylation, which results in transiently enhanced AKT signaling that may be linked to increases in cell survival and proliferation [3]. However, a direct relationship between transiently increased AKT kinase activity and TCL1 mediated transformation is not yet established and additional or alternative physiologic and/

* Corresponding author. Tel.: +1 310 206 6754; fax: +1 310 267 0382.
E-mail address: mteitell@ucla.edu (M.A. Teitell).

0304-3835/$ - see front matter © 2006 Elsevier Ireland Ltd. All rights reserved.
doi:10.1016/j.canlet.2006.07.006

or tumorigenic pathways and mechanisms for TCL1 activity remain a possibility.

A TCL–AKT interaction was identified in a yeast-two-hybrid screen for AKT binding proteins, and separately by co-immunoprecipitation, reasoning that TCL1 and AKT might act in the same signal transduction pathway since both proteins share the common ability to transform T cells [4,5]. A direct search for potential TCL1 interacting proteins, however, is not yet reported. Here, we performed TCL1 immunoprecipitation followed by mass spectrometry of TCL1 interacting proteins, which resulted in the identification of polynucleotide phosphorylase (PNPase) as a novel TCL1 binding partner. PNPase is an evolutionarily conserved 3′ to 5′ exoribonuclease whose transcription is induced by type I interferons [6] and is upregulated in terminally differentiated melanoma cells and in progeroid fibroblasts [7]. The binding domains on TCL1 for PNPase, and on PNPase for TCL1, were determined, and the impact of TCL1 on the RNA degrading activity of purified PNPase was evaluated. Molecular modeling provided several potential sites for interaction that were consistent with the biochemical data. Our results increase the spectrum of TCL1 binding proteins potentially involved in cellular homeostasis and malignant transformation beyond the AKT kinase family and may provide a link between TCL1 signal transduction and PNPase RNA processing pathways.

2. Materials and methods

2.1. Cell lines and tissue culture

Human Nalm-6 pre-B cells were a gift of D. Rawlings (University of Washington, Seattle, WA). HEK 293T cells were a gift from C. Denny (UCLA, Los Angeles, CA). Cells were maintained at 37 °C in 5% CO_2 in RPMI 1640 (Nalm-6) or MEM (HEK-293T) medium with 10% FBS, 2 mM L-glutamine, 1 mM sodium pyruvate, 0.1 mM non-essential amino acids, and antibiotics.

2.2. Antibodies

Antibodies used were against flag (Stratagene, La Jolla, CA), myc and mouse IgG (Santa Cruz Biotechnology, Santa Cruz, CA), TCL1 (27D6/20, a gift of M. Narducci, IDI-IRCCS, Rome, Italy), rabbit-HRP (Jackson ImmunoResearch Laboratories, West Grove, PA), and mouse-HRP and myc-HRP (Cell Signaling Technology, Beverly, MA). TCL1 antiserum has been previously described [8]. PNPase antiserum was generated at Biosource International (Hopkinton, MA). Rabbits were vaccinated with two keyhole limpet hemocyanin (KLH) linked peptides: Ac-LRREVGTSDKEILTSRIC-amide and Ac-CGRD PADGRMRLSRKVLQA-amide.

2.3. Plasmids and retroviruses

An MSCV-GFP-IRES-PURO retroviral expression vector was a gift of D. Rawlings. Flag-tagged TCL1 (MSCV-fTCL1-IRES-PURO) or untagged TCL1 (MSCV-TCL1-IRES-PURO) retroviral expression constructs were generated by PCR amplification of *TCL1* cDNA with end-modified primers, followed by cloning into MSCV-GFP-IRES-PURO to replace GFP (sequences available upon request). PNPase was obtained by PCR from a Nalm-6 pre-B cell cDNA library (primer sequences available upon request) and subcloned into the pCMV3-tag (Stratagene) myc-tagged mammalian expression vector. For full length and truncated forms of ^{35}S-labeled *in vitro*-translated PNPase, PNPase cDNA was cloned in frame into pCMV3-Tag with amino terminus primer 5′-ccggtaggatccATGGCGGCCTGCAGGTAC-3′ and either C2 5′-gcgcgcgtcgacGTTCATGATCTGTAATATC TCC-3′ or C1 5′-gcgcgcgtcgacACACCAG-TTTCTTTTA CC-3′ and carboxy primer 5′-ccgcatgtcgacTCACTGAGA ATTAGATG-3′ with either N1 5′-gcgcgcggatcc ACCAAGAGGACACCTCAG-3′ or N2 5′-gcgcgcgga tcc-CTATTTCAAAACCTCGAGC-3′. The integrity of all constructs was verified by sequencing.

Retroviral supernatants were produced by transient transfection of the 293T Phoenix packaging cell line (provided by G. Nolan, Stanford University, Stanford, CA). 10^5 Nalm-6 cells were infected in 1 ml of viral supernatant with 5 μg/ml of polybrene and selected in 1 μg/ml of puromycin. Puromycin-selected polyclonal populations were used in all experiments.

2.4. Immunoprecipitation and PNPase identification

All procedures were carried out at 4 °C. Cells were lysed using Triton X-100 lysis buffer (50 mM Tris, pH 7.4, 150 mM NaCl, 1 mM EDTA, and 1% Triton X-100) supplemented with protease inhibitors. Lysates were precleared with 30 μl of protein G-Plus (Santa Cruz Biotechnology) for 30 m and then incubated with 1–5 μg of immunoprecipitating antibody for 30 m followed by incubation with 50 μl of protein G-Plus–agarose for 2 h or overnight. Beads were washed five times using Triton X-100 lysis buffer and either separated by SDS–PAGE for Western blot or, for partner protein identification, eluted with 15 μg of Flag peptide in 0.5 M Tris HCl, pH 7.4 and 1.5 M NaCl followed by SDS–PAGE and staining with Silver Stain Plus (Bio-Rad, Hercules, CA) or Coomassie brilliant blue. An 85-kDa band was excised and analyzed by mass spectrometry. Sequence analysis was performed

at the Harvard Microchemistry Facility by microcapillary reverse-phase HPLC nano-electrospray tandem mass spectrometry (μLC/MS/MS) on a Finnigan LCQ DECA quadrapole ion trap mass spectrometer.

2.5. Western analysis

Western analysis was performed by standard techniques [9]. Briefly, samples were separated by SDS–PAGE, transferred to a nitrocellulose membrane, incubated with primary antibody overnight and then washed for 3 m six times in TBST. Then, a membrane was incubated in anti-rabbit^{-} HRP in TBST (diluted 1:5000) for 1 h, followed by six washes in TBST and developing with ECL+Plus reagent (Amersham-Pharmacia, Piscataway, NJ).

2.6. GST fusion protein pulldown assays

GST, GST–TCL1, or GST–PNPase fusion protein pulldown assays with wild type or truncated ^{35}S-labeled (Amersham Pharmacia) PNPase were performed by *in vitro* transcription/translation of PNPase using the TNT T3 Coupled Reticulocyte Lysate System (Promega, Madison, WI). GST, GST–TCL1, GST–TCL1-mutant, or GST–PNPase proteins were generated by transformation of BL21(DE3)lysS *Escherichia coli* (Invitrogen, Carlsbad, CA) with the pGEX6p-2T vector (Amersham-Pharmacia) or pGEX6p-2T containing TCL1, TCL1-mutant [10], or PNPase cDNAs, and purified as described by the manufacturer. Radiolabeled PNPase was incubated with 20 μg of GST, GST–TCL1, GST–TCL1-mutant, or GST–PNPase for 3 h. Glutathione–Sepharose 4B beads (Amersham-Pharmacia) with bound GST fusion proteins were pelleted and washed with Triton X-100 lysis buffer. Pulldowns were resolved on SDS–PAGE, fixed in 40% methanol/10% acetic acid for 30 m and immersed in Amplify (Amersham Pharmacia) for 30 m, dried, and exposed to film overnight. Coomassie brilliant blue staining demonstrated equal loading of full length and truncated ^{35}S-labeled PNPase.

2.7. mRNA degradation assay

Human PNPase was expressed as a GST fusion protein in BL21(DE3)lysS *E. coli* (Invitrogen) using the pGEX6p-2T vector (Amersham-Pharmacia). GST was removed from recombinant PNPase using PreScission Protease (Amersham-Pharmacia) for 16 h at 4 °C and recombinant PNPase purified by standard procedures. The pCY2-GAPDH plasmid, a gift of C.-Y. Chen (University of Alabama, Birmingham, AL) was cut with either *Eco*RI or *Xho*I to yield a linearized plasmid with or without a poly(A)$^{+}$ tail, respectively. Generation of RNA substrates and the *in vitro* RNA degradation assay was performed as previously described [11].

2.8. Modeling of TCL1–PNPase interaction

A structural model of human PNPase (UniProtKB/Swiss-Prot entry Q8TCS8) [12,13] was generated using the structure of the homologous PNPase from *Streptomyces antibioticus* (PDB entry 1E3P) [14,15]. The BLAST algorithm [16] was used to identify additional homologues of human PNPase. Multiple sequence alignments of PNPase were generated with clustalw [17] and the 3D-PSSM server [18]. Sequence alignments between human and *S. antibioticus* PNPase (UniProtKB/TrEMBL entry Q8CJQ6) [12,13], based on both algorithms, were manually edited to move gaps from α-helices and β-sheets to loop regions. Structural models of residues 38–744 were built with MODELLER version 6 [19–21]. A single model was selected based on structure validation with PROCHECK [22] and the WHAT IF web server [23,24]. The homology model was superimposed on the trimeric structure of PNPase from *S. antibioticus* (PDB entry 1E3P) (14) to generate a trimer model with the program lsqman [25].

Docking of monomeric and dimeric TCL1 (PDB entry 1JSG) [14,26] with the trimeric model of human PNPase was performed using the 3D-Dock suite of programs. Multiple starting orientations of TCL1 were generated with the randomspin program. The ftdock program was used to generate an ensemble of complexes [27]. Pair potential scoring was performed using rpscore [28], complexes were filtered using the filter program, and side chains were refined with multidock [29]. The clustering of complexes was observed using the center program. Pymol (http://www.pymol.org) was used to study models and generate figures (PyMOL Molecular Graphics System, DeLano Scientific, San Carlos, CA).

3. Results

3.1. Identification of PNPase as a novel TCL1 interacting protein

TCL1 and AKT-expressing Nalm-6 pre-B cells were infected with retroviruses expressing either a flag-epitope tagged or untagged (control) TCL1 cDNA. Whole cell extracts from flag-TCL1 or TCL1 expressing Nalm-6 cells were immunoblotted with either an anti-TCL1 or anti-flag antibody to establish the generation of stable polyclonal test and control cell populations (Fig. 1A). Following this, lysates were immunoprecipitated with an anti-flag antibody, with the bead-bound flag-tagged TCL1 protein eluted with excess flag peptide into the supernatant along with any co-immunoprecipitating protein complexes. With this approach, endogenous TCL1 was isolated and identified, as expected (data not shown). Immunoprecipitation also resulted in the isolation of an 85-kDa band on silver staining that was present in the flag-TCL1 expressing but absent in the control TCL1 transfectant Nalm-6

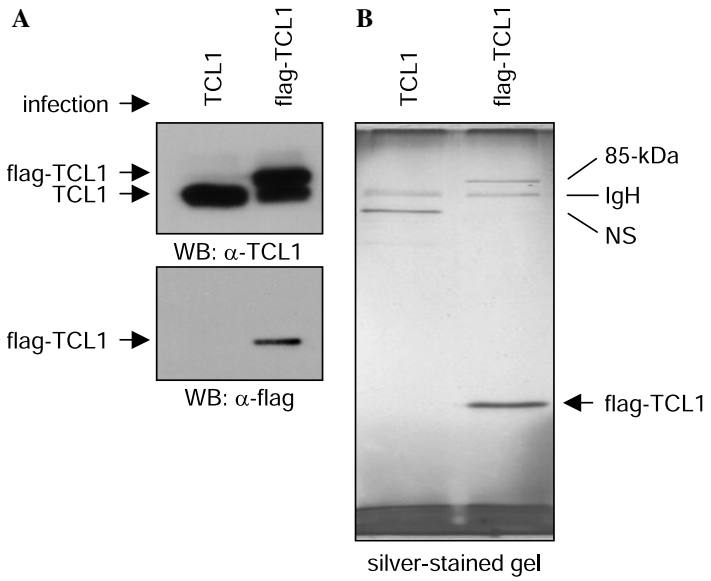

Fig. 1. Identification of a TCL1–PNPase interaction. (A) Nalm-6 pre-B cells were infected with TCL1 or flag-TCL1 expressing retroviruses, selected with puromycin, and analyzed by immunoblot using either TCL1 antiserum (upper panel) or flag antibody (lower panel). Bands corresponding to flag-TCL1 and TCL1 are indicated. (B) Flag immunoprecipitation of TCL1 or flag-TCL1 infected Nalm-6 pre-B cells was followed by washing and complex elution with excess flag peptide competitor. Eluates were resolved by SDS–PAGE and silver stained. A subsequent gel was stained with Coomassie brilliant blue and the 85-kDa band was excised and analyzed by mass spectrometry to identify a candidate TCL1–PNPase interaction.

cell lysates (Fig. 1B). Isolation of this single 85-kDa co-immunoprecipitating band has been repeated >10 times with identical results. Likewise, this single 85-kDa band has been repeatedly co-immunoprecipitated from TCL1-negative Jurkat T and Daoy medulloblastoma cell lines stably expressing flag-TCL1 (data not shown). In order to identify this 85-kDa TCL1-interacting protein, a large-scale assay was performed to generate sufficient amounts of the 85-kDa band to visualize by standard Coomassie gel staining (data not shown). The 85-kDa band was excised and analyzed by microcapillary reverse-phase HPLC nano-electrospray tandem mass spectrometry (μLC/MS/MS). A total of 118 peptide fragments identified by mass spectrometry matched sequences predicted to occur in the 85-kDa human PNPase 3′ to 5′ exoribonuclease and covered >85% of the translated sequence.

3.2. Establishment of a TCL1 interaction with PNPase

Once PNPase was identified as a TCL1 binding candidate by mass spectrometry, its cDNA was cloned from a Nalm-6 pre-B cell cDNA library. Sequencing established that the isolated clone was identical to the human mRNA for PNPase (GenBank AJ458465, gi:20372921). In order to independently verify the interaction between TCL1 and PNPase, the PNPase cDNA was subcloned into the pCMV3-tag mammalian expression vector to generate PNPase with a 3′-myc tag. HEK-293T cells were transiently transfected with MSCV-fTCL1-IRES-PURO and/or pCMV–PNPase-myc expression constructs. Immunoprecipitation performed with an anti-flag antibody followed by immunoblotting with an anti-myc antibody independently verified a TCL1–PNPase interaction with the tagged exogenous expression constructs (Fig. 2A). For unknown reasons it was not possible to detect a TCL1–PNPase interaction with an anti-myc antibody followed by an immunoblot with anti-flag antibody (data not shown).

To further establish the TCL1–PNPase interaction, antiserum against PNPase was generated by rabbit immunization with two KLH-linked PNPase peptides. Evaluation of the PNPase antiserum showed that it specifically detected a 114-kDa GST–PNPase fusion protein expressed and purified from bacteria (Fig. 2B) and also detected ~85-kDa, myc-tagged PNPase exogenously expressed in HEK-293T cells (data not shown). PNPase antiserum also established the identity of the 85-kDa band as PNPase when it was used to immunoblot the flag immunoprecipitation of MSCV-fTCL1-IRES-PURO-transfected HEK-293T cells (Fig. 2C). Finally, co-immunoprecipitation was performed with the 27D6/20 TCL1 monoclonal antibody [30] using Nalm-6 pre-B cells that naturally express TCL1; PNPase immunoblot of this co-immunoprecipitation established the existence of an endogenous interaction between TCL1 and PNPase in Nalm-6 pre-B cells (Fig. 2D). Attempts to perform the reverse co-immunoprecipitation with anti-PNPase antiserum have not identified TCL1, similar to the situation for flag-tagged constructs, for unknown reasons (data not shown).

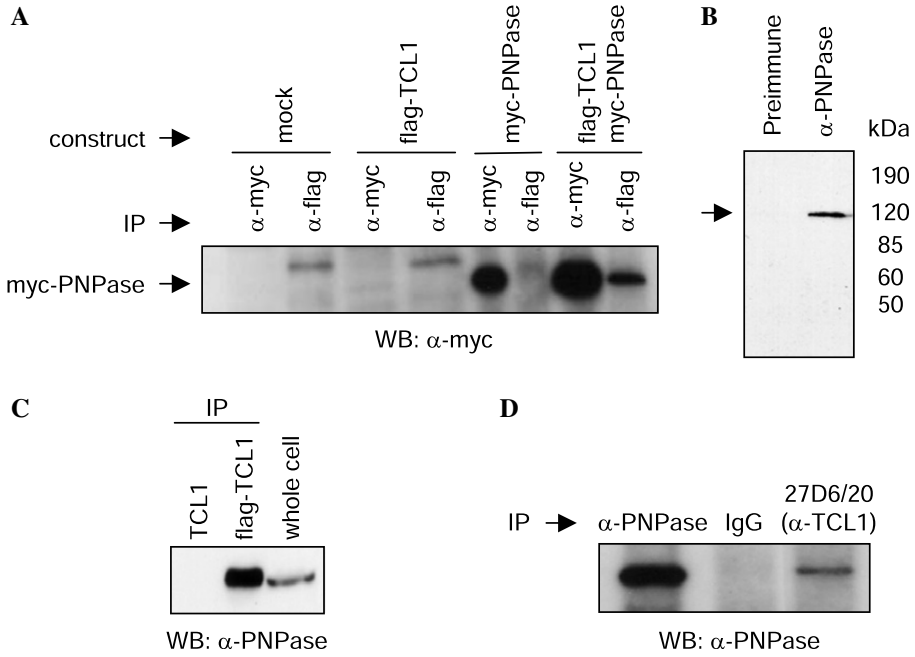

Fig. 2. Establishment of a TCL1–PNPase complex. (A) HEK-293T cells were transfected with a flag-TCL1 or myc-PNPase tagged expression construct or both. Cell lysates were immunoprecipitated (IP) with either α-myc or α-flag antibodies, resolved by SDS–PAGE, and analyzed by immunoblot with a myc antibody. (B) PNPase antiserum was developed by rabbit vaccination with two different conjugated peptides. Pre-immune and PNPase antiserum were assessed by immunoblot of a bacterially expressed 114-kDa GST–PNPase fusion protein separated by SDS–PAGE in each lane of the gel. (C) Proteins from flag immunoprecipitation reactions of TCL1 or flag-TCL1 infected Nalm-6 pre-B cells from Fig. 1B were immunoblotted with PNPase antiserum. (D) Uninfected Nalm-6 pre-B cell lysates were immunoprecipitated with α-PNPase antiserum, a monoclonal TCL1 antibody (27D6/20), or control mouse IgG and immunoblotted using PNPase antiserum.

3.3. The AKT binding domain of TCL1 interacts with the RNase PH domains of PNPase

TCL1 forms a novel β-barrel structure bounded by two four-stranded β-chain sheets connected by a long looping strand [26]. One four-stranded face of the TCL1 β-barrel provides a homodimerization domain for a second TCL1 protein, while the second four-stranded face provides a tryptophan-rich hydrophobic patch for binding to the pleckstrin homology (PH) domain of AKT family proteins [4,5]. Prior to this work, no other protein binding partners have been reported for TCL1.

Human PNPase is a multisubunit protein composed of two RNase PH domains separated by a α-helix and two carboxy-terminal RNA binding domains, KH and S1 [31]. Structural studies have shown that *S. antibioticus* PNPase forms a homotrimer, with a central cavity forming the probable site of catalytic activity, and six RNase PH domains flanked by extensions that contain KH and S1 domains [15]. A stacked PNPase trimer–dimer structure, creating a cylinder with an elongated central cavity, most likely exists in plants [32,33]. Human PNPase shows 34% amino acid sequence identity with bacterial PNPase and an even higher degree of sequence conservation in all of the key functional domains, suggesting a similar trimer or trimer–dimer conformation as seen in bacterial and plant homologues [31,33].

To identify which protein domains were responsible for a TCL1–PNPase interaction, a GST–TCL1-fusion protein pulldown assay was developed. Wild type and mutant GST–TCL1 fusion proteins have been described previously [10]. Pulldown assays demonstrated that GST–TCL1 interacts directly with *in vitro* translated PNPase with high affinity (Fig. 3A), as 5–10% of the total ^{35}S-labeled input PNPase was reproducibly bound to GST–TCL1 in these assays. This *in vitro* pulldown assay further supports the existence of an interaction between TCL1 and PNPase. Additionally, full length GST–PNPase fusion protein was able to bind *in vitro* translated and ^{35}S-labeled PNPase to a lesser extent (Fig. 3A), which was compatible with PNPase multimerization and consistent with the existence of a PNPase homomultimer in bacteria and plants [32].

PNPase deletion mutants were generated to establish which PNPase domain(s) is required for binding to TCL1 (Fig. 3B). GST–TCL1 bound ~25% of mutant PNPase molecules that contained either RNase PH domain (N2 or C1) compared to the amount of full length

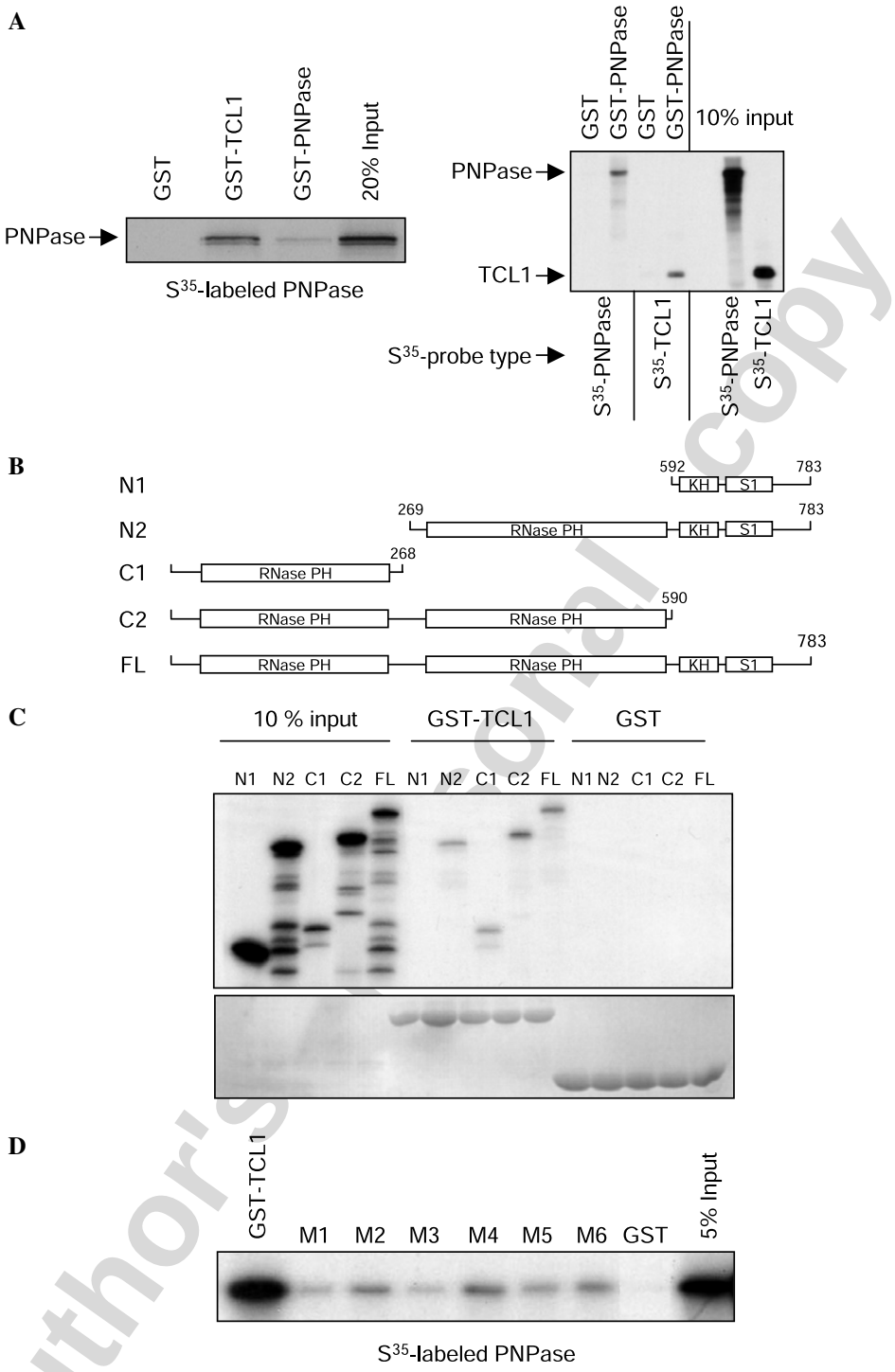

Fig. 3. Determining the interaction domains on PNPase and TCL1 for TCL1–PNPase complex formation. (A) ^{35}S-labeled PNPase was incubated with GST, GST–TCL1, or GST–PNPase recombinant proteins, bound to glutathione-sepharose beads, washed, boiled, resolved by SDS–PAGE, and exposed to film. (B) Depiction of PNPase full length (FL) and truncation constructs N1, N2, C1, and C2 generated for GST fusion protein pulldown analyses. RNase PH repeat domains and KH and S1 domains are indicated, along with amino acid numbers terminating each construct. The right column indicates the binding of each truncated PNPase species relative to full length PNPase from panel C. Binding for each construct was determined by the ratio of binding to input using densitometry. (C) GST fusion protein pulldown assays were performed with ^{35}S-labeled full length (FL) PNPase or sequential amino (N1, N2) or carboxy (C1, C2) terminal PNPase truncation mutants. The upper panel shows the autoradiograph of a typical experiment. The lower panel shows a Coomassie brilliant blue stain of the same gel to demonstrate equal GST–TCL1 or GST protein loading. (D) Point mutations in the βE (M1–M3) or βA (M4–M6) strands of TCL1 (10) impair the formation of a TCL1–PNPase complex using a GST–TCL1 fusion protein pulldown assay. Shown is wild type GST–TCL1, mutants 1–6, GST control, and 5% of the ^{35}S-labeled PNPase input for each reaction. Coomassie brilliant blue staining demonstrated equal fusion protein loading in each lane (data not shown).

(FL) PNPase bound (Fig. 3C). The linked KH and S1 domains (N1) failed to interact with GST–TCL1, while the PNPase deletion mutant with the KH and S1 domains removed (C2) bound GST–TCL1 as effectively as full length (FL) PNPase. These data indicate that the RNA binding KH and S1 domains are dispensable for PNPase interactions with TCL1. As such, TCL1 is the first protein shown to interact with the RNase PH repeat domains of PNPase. Lastly, a roughly twofold enhanced pulldown is observed when GST–TCL1 interacts with PNPase containing both RNase PH domains, suggesting a possible interaction synergy.

Six unique sets of point mutations, three each in the βA and βE strands of the TCL1 hydrophobic patch, disrupt the interaction of TCL1 with AKT [10]. These TCL1 mutants maintain their overall β-barrel structure as assessed by circular dichroism and were evaluated for interactions with full length PNPase using the GST–TCL1 fusion protein pulldown assay. As was the case for AKT, these TCL1 mutations interfered with PNPase binding to TCL1 (Fig. 3D). The data indicate that the AKT binding domain on TCL1 is also the site for binding to the RNase PH domains of PNPase and provide the first non-AKT family member interaction for TCL1.

3.4. Preferential poly(A)$^+$ RNA processing by PNPase is not altered by TCL1

Plant PNPase functions as a 3′ to 5′ exoribonuclease with a strong preference for polyadenylated RNA transcripts, probably due to a high affinity poly(A) binding site in the carboxy S1 domain, which is conserved in human PNPase [34,35]. Exogenous over-expression of human PNPase causes MYC and Bcl-xL downregulation [36,37], although the precise mechanism for this PNPase effect remains unknown. Exogenously expressed human PNPase localizes to the cytosol and mitochondria [7,36] and levels of mitochondria RNA, which have short poly(A) tails, are mostly unaffected by PNPase knockdown ([38] and Chen, et al., unpublished results). Since TCL1 binds PNPase (Figs. 2 and 3), purified recombinant human PNPase was evaluated for its ability to degrade RNA transcripts in the presence or absence of TCL1 (Fig. 4). Similar to its plant homologue, mammalian PNPase preferentially degraded poly(A)-containing GAPDH transcripts, with self-termination yielding a residual transcript similar in size to that of unprocessed GAPDH transcripts that lack a poly(A) sequence (Fig. 4A). Concurrent addition or pre-incubation of TCL1 did not change the rate of PNPase-mediated RNA degradation

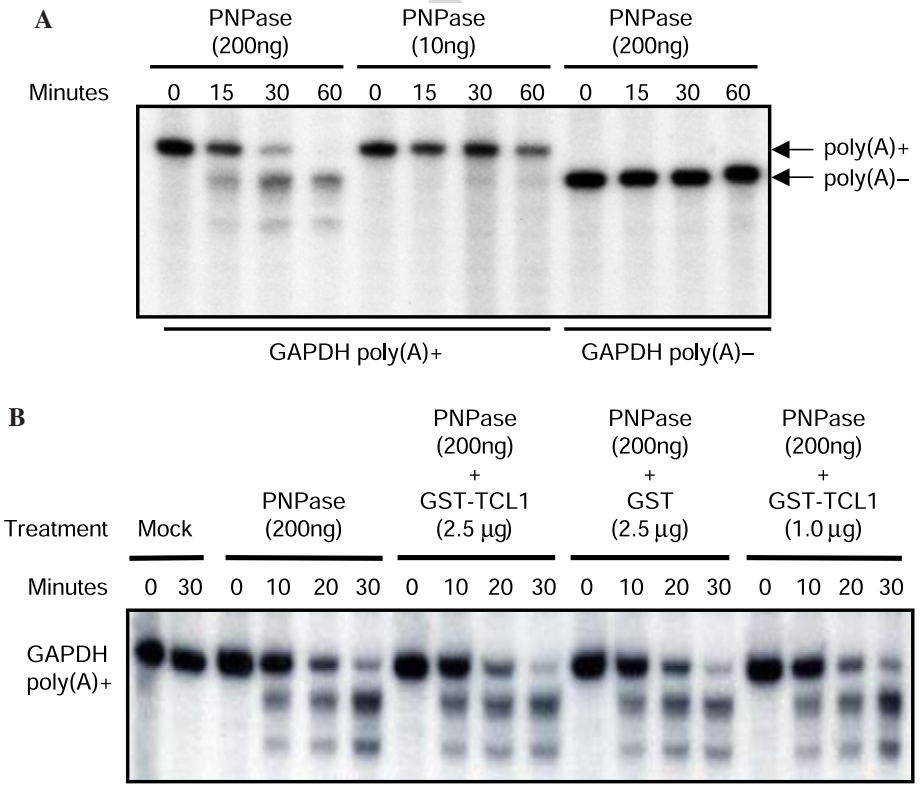

Fig. 4. Preferential poly(A)$^+$ RNA processing by PNPase is not altered by TCL1. (A) Purified recombinant PNPase or control GST alone was incubated with either poly(A)$^+$ or non-poly(A) GAPDH radiolabeled RNA for 0, 15, 30 or 60 m at 37 °C. Samples were resolved by acrylamide/urea gel electrophoresis followed by autoradiography. (B) Addition of GST (control) or GST–TCL1 fusion protein to the RNA degrading reaction did not alter the PNPase processing rate or pattern of resultant products.

nor was the preference from a poly(A)-containing sequence altered when compared to reactions that lacked added TCL1 (Fig. 4B and data not shown). Together, the data indicate a strong poly(A) preference for PNPase transcript processing and no effect on this processing activity for added TCL1.

3.5. Structure based identification of potential TCL1–PNPase interaction domains

A docking site(s) for a TCL1–PNPase interaction that was consistent with the interaction and processing data was sought. To do this, homology models of human PNPase were created first using the program MODELLER [19–21]. With 34% sequence identity to its homologue in *S. antibioticus*, there were variations possible in some parts of the sequence alignment. 3D-PSSM was used to help align the sequences using structural data [18]. One model was chosen for docking experiments based on structural criteria calculated by WHAT IF [23,24] and PROCHECK [22].

Three docking models for the interaction of a TCL1 dimer and a human PNPase trimer were generated. From the PNPase truncation and TCL1 mutant binding results (Fig. 3C and D), docking models were expected to have an interaction involving residues W19, W21, Q77, and Y79 of TCL1 [10] and either RNase PH domain 1 (residues 38–268) or RNase PH domain 2 (residues 269–590) of PNPase. After filtering for complexes satisfying these interaction constraints with a maximum distance of 6 Å, there were ~50 docking solutions for each PNPase molecule in the trimer. Visual inspection of the models demonstrated that multiple binding sites were possible. However, based on loose clustering of the TCL1 molecules docked on the trimer and the residue pairwise potential score [28] for each complex, three modes of interaction seemed most plausible. Table 1 shows the residue pairwise potential for the top 10 docking models predicted by rigid body docking. Side chain refinement suggested one representative model for each binding mode. Fig. 5A shows two predicted interactions. The top scoring model (Fig. 5A, red) interacts with RNase PH domain 2, specifically with α-helix 12 and β-sheet 19, as previously defined for *S. antibioticus* PNPase [15]. The third best model (Fig. 5A, blue) before and after side chain refinement interacts with α-helix 5 and β-sheets 1 and 2 of RNase PH domain 1. Model 5 from the rigid body search (the second top scoring model after side chain refinement) interacts with α-helix 5 and α-helix 12, creating an interaction with both RNase PH domains; Fig. 5B shows the region of PNPase that interact with TCL1 in this binding mode.

4. Discussion

TCL1 expression in stage-specific B and T cells contributes to immune system development and function [39]. Chromosome rearrangements in early T lineage cells, and aberrant regulation by an unknown mechanism(s) in peripheral B cells, leads to dysregulated TCL1 expression and mature B and T cell cancers, although the TCL1 transforming mechanism remains unresolved (reviewed in [1]). Formation of a multimeric TCL1–AKT complex with transiently enhanced AKT activation may account for its cellular and transforming activity, but additional TCL1-containing complexes remain possible. Supporting an alternative or additional mechanism, enhanced activation of AKT may be insufficient for transformation as mice with B cells deficient in Pten, a negative regulator of Akt, did not develop B cell lymphomas, and constitutively active Akt caused cell senescence rather than transformation [40,41].

Table 1
Docking results

Complex	RPscore (rigid body docking)	RPscore (after side chain refinement)	Area buried (Å^2)	Interaction domain
1	**2.580**	**2.750**	**777**	**RNase PH 2**
2	1.950	0.790	712	RNase PH1
3	**1.710**	**1.110**	**822**	**RNase PH 1**
4	1.540	0.110	877	BOTH
5	**1.400**	**1.360**	**1175**	**BOTH**
6	1.040	−0.120	741	RNase PH 1
7	1.000	0.630	1017	RNase PH 2
8	1.000	−2.670	1068	BOTH
9	0.700	−0.950	897	RNase PH 2
10	0.600	0.180	1006	RNase PH 2

The residue–residue pair potential, RPscore, is calculated by rpscore in the 3D-Dock suite [28]. The complexes are ordered based on their pair potential score after rigid body docking. Area buried was calculated using areaimol in the ccp4 program suite [57]. The interaction domain is the RNase PH domain with which TCL1 has its primary interaction. The three best interaction models are in bold and shown in Fig. 5.

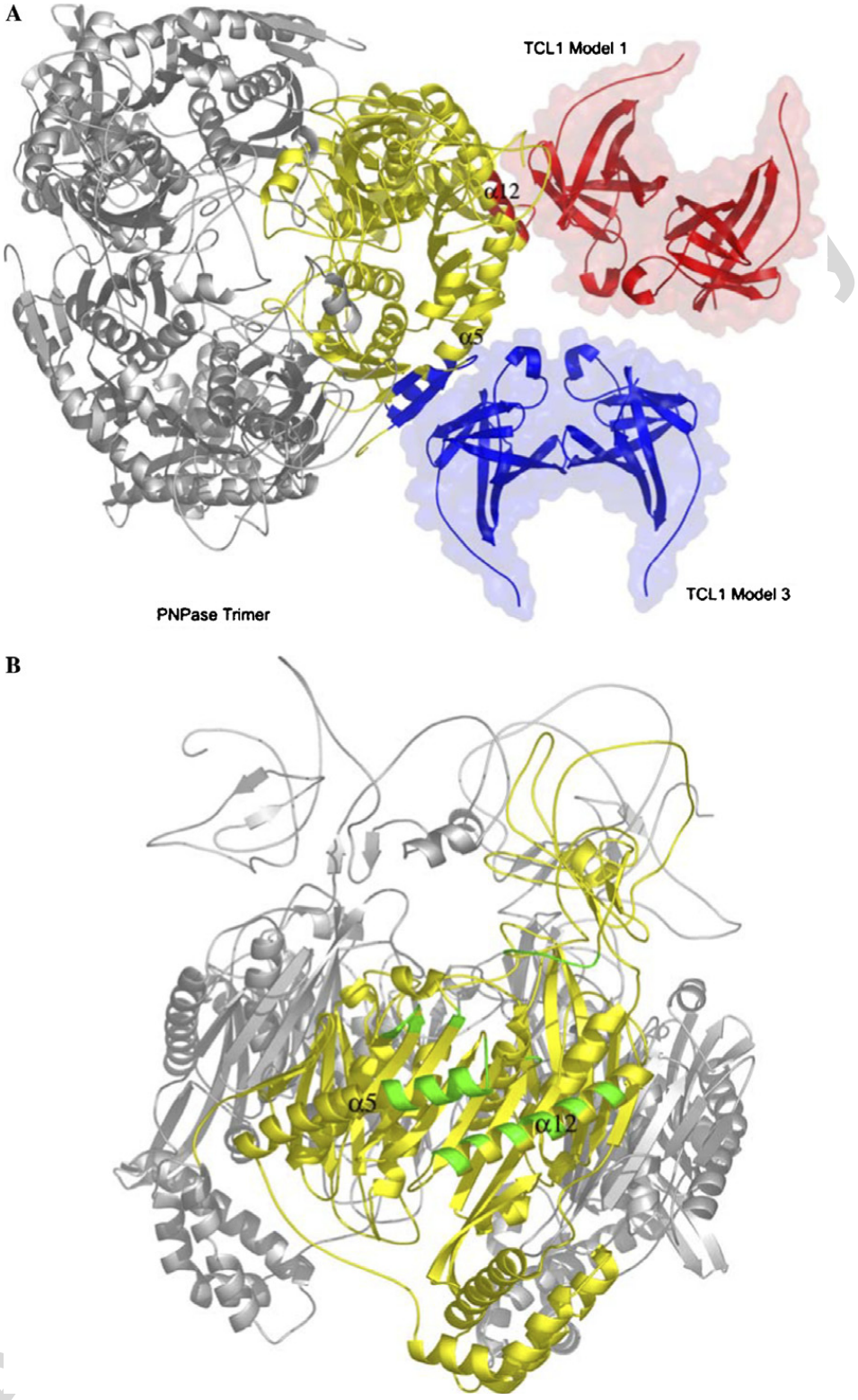

Fig. 5. Structure based identification of potential TCL1–PNPase interaction domains. (A) A view of the modeled PNPase trimer down the three-fold axis is shown. A monomer of PNPase interacting with two models of dimeric TCL1 is shown in yellow. The top-scoring model (see Table 1) is shown in red ribbon and surface representations. The amino acids that it interacts with on the RNase PH domain 2 of PNPase are also colored red. The third-scoring model, shown in blue, predicts that TCL1 interacts with the blue residues of the RNase PH domain 1 of PNPase. (B) After side chain refinement, the second-scoring model for an interaction of TCL1 with PNPase includes both RNase PH domains 1 and 2. This model is demonstrated with a view of the TCL1 docking site on the PNPase trimer perpendicular to the three-fold axis. For clarity, only PNPase is shown. The residues of PNPase that are involved in this interaction with TCL1 are colored green. (For interpretation of the references to colour in this figure legend, the reader is referred to the web version of this paper.)

Since a survey for TCL1 interacting proteins has not been reported, we examined Nalm-6 pre-B cells using TCL1 immunoprecipitation followed by mass spectrometry analysis. Nalm-6 is an ideal cell type to study since there is abundant TCL1 and AKT and identification of a TCL1–AKT complex was anticipated. Surprisingly, a TCL1–PNPase but not a TCL1–AKT complex was detected, even when immunoprecipitated proteins were analyzed for bound AKT by immunoblot (data not shown). Epitope-tagged and endogenous TCL1–TCL1 (data not shown) and TCL1–PNPase complexes were confirmed *in vivo*, while *in vitro* translated PNPase was captured with a GST–TCL1 fusion protein pulldown assay, suggesting a direct interaction. The RNase PH domains on PNPase and the AKT binding domain on TCL1 were identified as TCL1–PNPase interaction sites. Several docking models for a TCL1–PNPase complex were developed that were consistent with the binding data and exclusion of TCL1 from the linked KH and S1 RNA binding and catalytic core domains of PNPase. From this unbiased search, we conclude that TCL1 preferentially interacts with PNPase compared with other proteins expressed in human B cells using multiple assay systems.

PNPase is an evolutionarily conserved 3′ to 5′ exonuclease that is related to RNase PH and which degrades RNA in bacteria and plants [42]. In bacteria, PNPase is a component of the multiprotein RNA degrading complex called the degradosome which also contains RNase E, and the DEAD-box RNA helicase RhlB [43–45]. In plants, PNPase is located in the chloroplast where it regulates RNA turnover and poly(A) tail addition to transcripts [32,34,46–48]. Thus far, interacting proteins for human PNPase have not been identified and PNPase likely exists independently from a mammalian degradosome or exosome equivalent.

Modeling the interaction of TCL1 and PNPase first required a model of human PNPase to combine with the solved structure of TCL1 [26]. Success in structural modeling has been achieved using homology techniques [49,50] and, since human PNPase has 34% sequence identity to *S. antibioticus* PNPase, a reasonable structural model was created with MODELLER. For docking, experimental constraints were considered, and modeled interactions tended to cluster in a few potential areas. Interestingly, the top scoring models for three distinct clusters of docking suggest that PNPase may present an interaction surface to TCL1 that is similar to the surface presented by the AKT PH domain, which was based on the interaction footprinting between TCL1 and AKT [2]. The modeled interaction therefore predicts key residues on PNPase for interaction with TCL1, similar to modeling results that predicted key residues on TCL1 for interacting with AKT [10,51]. The orientation of TCL1 determines whether it can be involved in one or two interactions with PNPase, AKT, or other proteins, although the lack AKT by immunoblot from the TCL1 immunoprecipitation suggests against a TCL–AKT–PNPase complex. There is a possibility that TCL1 can bring together a high local concentration of PNPase molecules, but steric hindrance beyond the docking models may preclude this occurrence.

Accounting for molecular flexibility is not easily done in modeling proteins and especially in docking two proteins. For example, errors in sequence alignment can lead to large errors in homology models [52]. Also, problems arising from the structural differences of proteins in the bound versus unbound state have been described [50]. If either TCL1 or PNPase undergoes a large structural change upon binding, it would make rigid body docking less likely to predict accurate models for interaction. We have presented three structural models for the interaction of TCL1 with PNPase that account for the interaction of TCL1 with either RNase PH domain and a third interaction of a TCL1 molecule with both of the RNase PH domains at the same time. The first two models suggest how TCL1 can bind to constructs N2 and C1 in isolation (Fig. 3). The increase in binding with the full protein compared to either RNase PH domain alone may be due to cooperative binding between RNase PH domains in a PNPase molecule or multimeric assembly or it may be due to a stronger binding interface created by the presence of both RNase PH domains that is demonstrated in the third model.

TCL1 bound the PNPase RNase PH repeat domains but did not interact with the KH and S1 RNA binding motifs and did not affect the poly(A)$^+$ GAPDH degradation rate or pattern *in vitro*. Therefore, despite providing a first interaction for human PNPase, and a non-AKT family interaction for TCL1, the biological implications for a TCL1–PNPase complex remain to be determined. Some insight into the complexity of this problem is provided by the observation that endogenous GAPDH mRNA expression was selectively maintained at a relatively constant level in several cell types overexpressing large amounts of exogenous human

PNPase [36,53]. The stability of certain mammalian mRNAs is regulated by stimuli-responsive cis-RNA elements, including AU-rich elements (AREs) that are present on 3′ message termini (reviewed in [54]). *In vivo*, a TCL1 interaction may therefore still modulate PNPase activity by additional interactions with factors not present on *in vitro* synthesized transcripts. Alternatively, TCL1 may participate in regulating PNPase enzyme levels, which can also be quite complicated, as recent findings indicate either a proportional increase or no increase in PNPase protein expression with β-interferon induced PNPase transcription in melanoma cells [6,37,55]. Since TCL1 expression is pro-growth and survival [3,4,56], and exogenous PNPase over-expression appears associated with cell senescence and differentiation [7,53], an intriguing possibility is that the biological significance for dysregulated TCL1 expression is to oppose PNPase effects during the promotion of malignant transformation.

Acknowledgements

This work was supported by NIH Grants T32CA09056 (S.W.F.), T32CA009120 (D.W.D. and C.E.B.), F31HD041889 (R.N.R.), R21GM61721 and R01GM073981 (C.M.K.), R01CA90571 and R01CA107300 (M.A.T.), and by the UCLA-IGERT bioinformatics traineeship NSF DGE-9987641 (S.A.S.), the Muscular Dystrophy Association 03018774 (C.M.K.), and CMISE, a NASA URETI Institute NCC 2-1364 (M.A.T.). C.M.K. is a Beckman Scholar and M.A.T. is a Scholar of the Leukemia and Lymphoma Society.

References

[1] M.A. Teitell, The TCL1 family of oncoproteins: co-activators of transformation, Nat. Rev. Cancer 5 (2005) 640.
[2] D. Auguin, P. Barthe, C. Royer, M.H. Stern, M. Noguchi, S.T. Arold, C. Roumestand, Structural basis for the co-activation of protein kinase B by T-cell leukemia-1 (TCL1) family proto-oncoproteins, J. Biol. Chem. 279 (2004) 35890.
[3] K.K. Hoyer, S.W. French, D.E. Turner, M.T. Nguyen, M. Renard, C.S. Malone, S. Knoetig, C.F. Qi, T.T. Su, H. Cheroutre, R. Wall, D.J. Rawlings, H.C. Morse 3rd., M.A. Teitell, Dysregulated TCL1 promotes multiple classes of mature B cell lymphoma, Proc. Natl. Acad. Sci. USA 99 (2002) 14392.
[4] J. Laine, G. Kunstle, T. Obata, M. Sha, M. Noguchi, The protooncogene TCL1 is an Akt kinase coactivator, Mol. Cell 6 (2000) 395.
[5] Y. Pekarsky, A. Koval, C. Hallas, R. Bichi, M. Tresini, S. Malstrom, G. Russo, P. Tsichlis, C.M. Croce, Tcl1 enhances Akt kinase activity and mediates its nuclear translocation, Proc. Natl. Acad. Sci. USA 97 (2000) 3028.
[6] M. Leszczyniecka, Z.Z. Su, D.C. Kang, D. Sarkar, P.B. Fisher, Expression regulation and genomic organization of human polynucleotide phosphorylase, hPNPase(old-35), a Type I interferon inducible early response gene, Gene 316 (2003) 143.
[7] M. Leszczyniecka, D.C. Kang, D. Sarkar, Z.Z. Su, M. Holmes, K. Valerie, P.B. Fisher, Identification and cloning of human polynucleotide phosphorylase, hPNPase old-35, in the context of terminal differentiation and cellular senescence, Proc. Natl. Acad. Sci. USA 99 (2002) 16636.
[8] M. Teitell, M.A. Damore, G.G. Sulur, D.E. Turner, M.H. Stern, J.W. Said, C.T. Denny, R. Wall, TCL1 oncogene expression in AIDS-related lymphomas and lymphoid tissues, Proc. Natl. Acad. Sci. USA. 96 (1999) 9809.
[9] J.W. Said, K.K. Hoyer, S.W. French, L. Rosenfelt, M. Garcia-Lloret, P.J. Koh, T.C. Cheng, G.G. Sulur, G.S. Pinkus, W.M. Kuehl, D.J. Rawlings, R. Wall, M.A. Teitell, TCL1 oncogene expression in B cell subsets from lymphoid hyperplasia and distinct classes of B cell lymphoma, Lab Invest. 81 (2001) 555.
[10] S.W. French, R.R. Shen, P.J. Koh, C.S. Malone, P. Mallick, M.A. Teitell, A modeled hydrophobic domain on the TCL1 oncoprotein mediates association with AKT at the cytoplasmic membrane, Biochemistry 41 (2002) 6376.
[11] C.Y. Chen, R. Gherzi, J.S. Andersen, G. Gaietta, K. Jurchott, H.D. Royer, M. Mann, M. Karin, Nucleolin and YB-1 are required for JNK-mediated interleukin-2 mRNA stabilization during T-cell activation, Genes Dev. 14 (2000) 1236.
[12] R. Apweiler, A. Bairoch, C.H. Wu, W.C. Barker, B. Boeckmann, S. Ferro, E. Gasteiger, H. Huang, R. Lopez, M. Magrane, M.J. Martin, D.A. Natale, C. O'Donovan, N. Redaschi, L.S. Yeh, UniProt: the Universal Protein knowledgebase, Nucleic Acids Res. 32 (2004) D115.
[13] A. Bairoch, R. Apweiler, C.H. Wu, W.C. Barker, B. Boeckmann, S. Ferro, E. Gasteiger, H. Huang, R. Lopez, M. Magrane, M.J. Martin, D.A. Natale, C. O'Donovan, N. Redaschi, L.S. Yeh, The Universal Protein Resource (UniProt), Nucleic Acids Res. 33 (2005) D154.
[14] H.M. Berman, J. Westbrook, Z. Feng, G. Gilliland, T.N. Bhat, H. Weissig, I.N. Shindyalov, P.E. Bourne, The Protein Data Bank, Nucleic Acids Res. 28 (2000) 235.
[15] M.F. Symmons, G.H. Jones, B.F. Luisi, A duplicated fold is the structural basis for polynucleotide phosphorylase catalytic activity, processivity, and regulation, Structure Fold Des. 8 (2000) 1215.
[16] S.F. Altschul, W. Gish, W. Miller, E.W. Myers, D.J. Lipman, Basic local alignment search tool, J. Mol. Biol. 215 (1990) 403.
[17] J.D. Thompson, D.G. Higgins, T.J. Gibson, CLUSTAL W: improving the sensitivity of progressive multiple sequence alignment through sequence weighting, position-specific gap penalties and weight matrix choice, Nucleic Acids Res. 22 (1994) 4673.
[18] L.A. Kelley, R.M. MacCallum, M.J. Sternberg, Enhanced genome annotation using structural profiles in the program 3D-PSSM, J. Mol. Biol. 299 (2000) 499.
[19] A. Sali, T.L. Blundell, Comparative protein modelling by satisfaction of spatial restraints, J. Mol. Biol. 234 (1993) 779.

[20] A. Fiser, R.K. Do, A. Sali, Modeling of loops in protein structures, Protein Sci. 9 (2000) 1753.
[21] M.A. Marti-Renom, A.C. Stuart, A. Fiser, R. Sanchez, F. Melo, A. Sali, Comparative protein structure modeling of genes and genomes, Annu. Rev. Biophys. Biomol. Struct. 29 (2000) 291.
[22] R.A. Laskowski, D.S. Moss, J.M. Thornton, Main-chain bond lengths and bond angles in protein structures, J. Mol. Biol. 231 (1993) 1049.
[23] G. Vriend, WHAT IF: a molecular modeling and drug design program, J. Mol. Graph. 8 (1990) 52.
[24] R. Rodriguez, G. Chinea, N. Lopez, T. Pons, G. Vriend, Homology modeling, model and software evaluation: three related resources, Bioinformatics 14 (1998) 523.
[25] G.J. Kleywegt, Use of non-crystallographic symmetry in protein structure refinement, Acta. Crystallogr. D. Biol. Crystallogr. 52 (1996) 842.
[26] F. Hoh, Y.S. Yang, L. Guignard, A. Padilla, M.H. Stern, J.M. Lhoste, H. van Tilbeurgh, Crystal structure of p14TCL1, an oncogene product involved in T-cell prolymphocytic leukemia, reveals a novel beta-barrel topology, Structure 6 (1998) 147.
[27] H.A. Gabb, R.M. Jackson, M.J. Sternberg, Modelling protein docking using shape complementarity, electrostatics and biochemical information, J. Mol. Biol. 272 (1997) 106.
[28] G. Moont, H.A. Gabb, M.J. Sternberg, Use of pair potentials across protein interfaces in screening predicted docked complexes, Proteins 35 (1999) 364.
[29] R.M. Jackson, H.A. Gabb, M.J. Sternberg, Rapid refinement of protein interfaces incorporating solvation: application to the docking problem, J. Mol. Biol. 276 (1998) 265.
[30] M.G. Narducci, E. Pescarmona, C. Lazzeri, S. Signoretti, A.M. Lavinia, D. Remotti, E. Scala, C.D. Baroni, A. Stoppacciaro, C.M. Croce, G. Russo, Regulation of TCL1 expression in B- and T-cell lymphomas and reactive lymphoid tissues, Cancer Res. 60 (2000) 2095.
[31] R. Raijmakers, W.V. Egberts, W.J. van Venrooij, G.J. Pruijn, Protein-protein interactions between human exosome components support the assembly of RNase PH-type subunits into a six-membered PNPase-like ring, J. Mol. Biol. 323 (2002) 653.
[32] S. Baginsky, A. Shteiman-Kotler, V. Liveanu, S. Yehudai-Resheff, M. Bellaoui, R.E. Settlage, J. Shabanowitz, D.F. Hunt, G. Schuster, W. Gruissem, Chloroplast PNPase exists as a homo-multimer enzyme complex that is distinct from the Escherichia coli degradosome, RNA 7 (2001) 1464.
[33] M.F. Symmons, M.G. Williams, B.F. Luisi, G.H. Jones, A.J. Carpousis, Running rings around RNA: a superfamily of phosphate-dependent RNases, Trends Biochem. Sci. 27 (2002) 11.
[34] I. Lisitsky, A. Kotler, G. Schuster, The mechanism of preferential degradation of polyadenylated RNA in the chloroplast. The exoribonuclease 100RNP/polynucleotide phosphorylase displays high binding affinity for poly(A) sequence, J. Biol. Chem. 272 (1997) 17648.
[35] S. Yehudai-Resheff, V. Portnoy, S. Yogev, N. Adir, G. Schuster, Domain analysis of the chloroplast polynucleotide phosphorylase reveals discrete functions in RNA degradation, polyadenylation, and sequence homology with exosome proteins, Plant Cell 15 (2003) 2003.
[36] D. Sarkar, E.S. Park, L. Emdad, A. Randolph, K. Valerie, P.B. Fisher, Defining the domains of human polynucleotide phosphorylase (hPNPaseOLD-35) mediating cellular senescence, Mol. Cell. Biol. 25 (2005) 7333.
[37] D. Sarkar, E.S. Park, P.B. Fisher, Defining the mechanism by which IFN-beta dowregulates c-myc expression in human melanoma cells: pivotal role for human polynucleotide phosphorylase (hPNPase(old-35)), Cell Death Differ. (2006).
[38] T. Nagaike, T. Suzuki, T. Katoh, T. Ueda, Human mitochondrial mRNAs are stabilized with polyadenylation regulated by mitochondria-specific poly(A) polymerase and polynucleotide phosphorylase, J. Biol. Chem. 280 (2005) 19721.
[39] S.M. Kang, M.G. Narducci, C. Lazzeri, A.M. Mongiovi, E. Caprini, A. Bresin, F. Martelli, J. Rothstein, C.M. Croce, M.D. Cooper, G. Russo, Impaired T- and B-cell development in Tcl1-deficient mice, Blood 105 (2005) 1288.
[40] A. Suzuki, T. Kaisho, M. Ohishi, M. Tsukio-Yamaguchi, T. Tsubata, P.A. Koni, T. Sasaki, T.W. Mak, T. Nakano, Critical roles of Pten in B cell homeostasis and immunoglobulin class switch recombination, J. Exp. Med 197 (2003) 657.
[41] H. Miyauchi, T. Minamino, K. Tateno, T. Kunieda, H. Toko, I. Komuro, Akt negatively regulates the in vitro lifespan of human endothelial cells via a p53/p21-dependent pathway, Embo J. 23 (2004) 212.
[42] A.J. Carpousis, The *Escherichia coli* RNA degradosome: structure, function and relationship in other ribonucleolytic multienzyme complexes, Biochem. Soc. Trans. 30 (2002) 150.
[43] E. Blum, B. Py, A.J. Carpousis, C.F. Higgins, Polyphosphate kinase is a component of the *Escherichia coli* RNA degradosome, Mol. Microbiol. 26 (1997) 387.
[44] A. Miczak, V.R. Kaberdin, C.L. Wei, S. Lin-Chao, Proteins associated with RNase E in a multicomponent ribonucleolytic complex, Proc. Natl. Acad. Sci. USA 93 (1996) 3865.
[45] B. Py, C.F. Higgins, H.M. Krisch, A.J. Carpousis, A DEAD-box RNA helicase in the Escherichia coli RNA degradosome, Nature 381 (1996) 169.
[46] S. Baginsky, W. Gruissem, Endonucleolytic activation directs dark-induced chloroplast mRNA degradation, Nucleic Acids Res. 30 (2002) 4527.
[47] Q.S. Li, J.D. Gupta, A.G. Hunt, Polynucleotide phosphorylase is a component of a novel plant poly(A) polymerase, J. Biol. Chem. 273 (1998) 17539.
[48] S. Yehudai-Resheff, M. Hirsh, G. Schuster, Polynucleotide phosphorylase functions as both an exonuclease and a poly(A) polymerase in spinach chloroplasts, Mol. Cell. Biol. 21 (2001) 5408.
[49] R. Mendez, R. Leplae, M.F. Lensink, S.J. Wodak, Assessment of CAPRI predictions in rounds 3-5 shows progress in docking procedures, Proteins 60 (2005) 150.
[50] R. Mendez, R. Leplae, L. De Maria, S.J. Wodak, Assessment of blind predictions of protein-protein interactions: current status of docking methods, Proteins 52 (2003) 51.
[51] G. Kunstle, J. Laine, G. Pierron, S. Kagami Si, H. Nakajima, F. Hoh, C. Roumestand, M.H. Stern, M. Noguchi, Identification of Akt association and oligomerization domains of the Akt kinase coactivator TCL1, Mol. Cell Biol. 22 (2002) 1513.
[52] C. Venclovas, A. Zemla, K. Fidelis, J. Moult, Assessment of progress over the CASP experiments, Proteins 53 (Suppl. 6) (2003) 585.

[53] D. Sarkar, M. Leszczyniecka, D.C. Kang, I.V. Lebedeva, K. Valerie, S. Dhar, T.K. Pandita, P.B. Fisher, Down-regulation of Myc as a potential target for growth arrest induced by human polynucleotide phosphorylase (hPNPaseold-35) in human melanoma cells, J. Biol. Chem. 278 (2003) 24542.
[54] C.Y. Chen, A.B. Shyu, AU-rich elements: characterization and importance in mRNA degradation, Trends Biochem. Sci. 20 (1995) 465.
[55] K. Gewartowski, R. Tomecki, L. Muchowski, A. Dmochow Ska, A. Dzwonek, M. Malecki, H. Skurzak, J. Ostrowski, P.P. Stepien, Up-regulation of human PNPase mRNA by beta-interferon has no effect on protein level in melanoma cell lines, Acta. Biochim. Pol. 53 (2006) 179.
[56] K.K. Hoyer, M. Herling, K. Bagrintseva, D.W. Dawson, S.W. French, M. Renard, J.G. Weinger, D. Jones, M.A. Teitell, T cell leukemia-1 modulates TCR signal strength and IFN-gamma levels through phosphatidylinositol 3-kinase and protein kinase C pathway activation, J. Immunol. 175 (2005) 864.
[57] B. Lee, F.M. Richards, The interpretation of protein structures: estimation of static accessibility, J. Mol. Biol. 55 (1971) 379.